Geophys. J. Int. (2006) **167,** 467–478 doi: 10.1111/j.1365-246X.2006.03108.x

The methodology of quantification of volcanic explosions from broad-band seismic signals and its application to the 2004–2005 explosions at Volcán de Colima, Mexico

Vyacheslav M. Zobin,[1] Carlos Navarro,[1] Gabriel Reyes-Dávila,[1] Justo Orozco,[1] Mauricio Bretón,[1] Armando Tellez,[1] Gabriel Reyes-Alfaro[2] and Homero Vázquez[2]

[1]*Observatorio Vulcanológico, Universidad de Colima, Colima, Col.,* 28045, *Mexico. E-mail: vzobin@cgic.ucol.mx*
[2]*Facultad de Ciencias, Universidad de Colima, Colima, Col.,* 28045, *México*

Accepted 2006 June 13. Received 2006 June 12; in original form 2005 October 11

SUMMARY

A methodology is proposed for the quantification of volcanic explosions based on three parameters derived from broad-band seismic signals: the counter force of the eruption F, the power of the explosion P and the duration of the upward movement of the gas slug in the conduit to the free surface of magma, D. This methodology was applied to the 2004–2005 sequence of explosions at Volcán de Colima, Mexico. The broad-band records of more than 100 explosive events were obtained at a distance of 4 km from the crater. We determined the counter force of the eruption by modelling the low-frequency impulse of the seismic records of 66 volcanic explosions and estimated the power of 116 explosions from the spectra of the high-frequency impulse. The power of Colima explosions spans five orders of magnitude; the counter force spans four orders of magnitude. We show that the power of a volcanic explosion is proportional to the counter force of the eruption. These parameters may be used for the elaboration of a scale of volcanic explosions.

Key words: explosive earthquakes, explosive eruption, Volcán de Colima, volcanic seismology.

1 INTRODUCTION

Models proposed for volcanic explosions consider that they are produced by an unsteady flux of gas released from magma. The reviews by Cashman *et al.* (2000), Vergniolle & Mangan (2000) and Morrissey & Mastin (2000) describe the general features of magmatic fragmentation and models of explosive eruptions. Small bubbles move upward in the melt and grow driving the magma conduit system into oscillation. When the bubbles get close to the free surface of magma, they explode. This process generates seismic signals that may be used for the quantification of volcanic explosions.

The goal of quantifying the size of explosive volcanic eruptions has produced several magnitude and intensity scales, including the eight-grade Volcanic Explosivity Index, or VEI (Newhall & Self 1982; Carey & Sigurdsson 1989; Pyle 2000). These scales are based primarily on the volume of the resulting deposit and, as a result, their principal subdivisions cover large ranges of values (e.g. ranges in volume by about a factor of 10 for each VEI unit). In addition, they are commonly applied to the total products of an eruption, as opposed to those of specific phases during a related sequence of explosive events. An alternative approach to quantifying size is to use the seismic signals induced by volcanic explosions that has the potential advantage of discriminating between the magnitudes of events with greater precision.

By comparing estimations of the VEI (BGVN, 1980–2005) with the counter force of the eruption F estimated from the modelling of seismic signals (Kanamori *et al.* 1984; Nishimura & Hamaguchi 1993), it is shown that a better resolution of the explosion size is obtained using F. For the Popocatépetl eruption of 1997–1998, based on the total volume of emitted magmatic material, a value of only VEI $= 3$ was estimated. The seismic estimation of F allows the discrimination of the sequence of individual explosions whose counter forces vary within 1.5 orders. The 1983 Asama and the 1989 Tokachi explosive eruptions are both characterized by a value VEI $= 2$. The seismic estimation of F shows that the Asama explosion was stronger than the Tokachi explosions.

The development of digital broad-band seismic instrumentation at volcanoes has allowed the recording of good-quality seismic signals associated with volcanic explosions (Kawakatsu *et al.* 1992; Neuberg *et al.* 1994; Rowe *et al.* 1998; Johnson *et al.* 1998; Aster *et al.* 2003, among others). Fig. 1 shows a typical broad-band seismic record of a Vulcanian explosion at Volcán de Colima, Mexico. This unfiltered signal consists of two impulses, of low-frequency (LF) and high-frequency (HF) contents.

Broad-band observations (Neuberg *et al.* 1994; Rowe *et al.* 1998; Chouet *et al.* 2003, 2005) have revealed also the presence of very-long-period (VLP) seismic signals associated with small-scale degassing at volcanoes. These signals were reported from broad-band

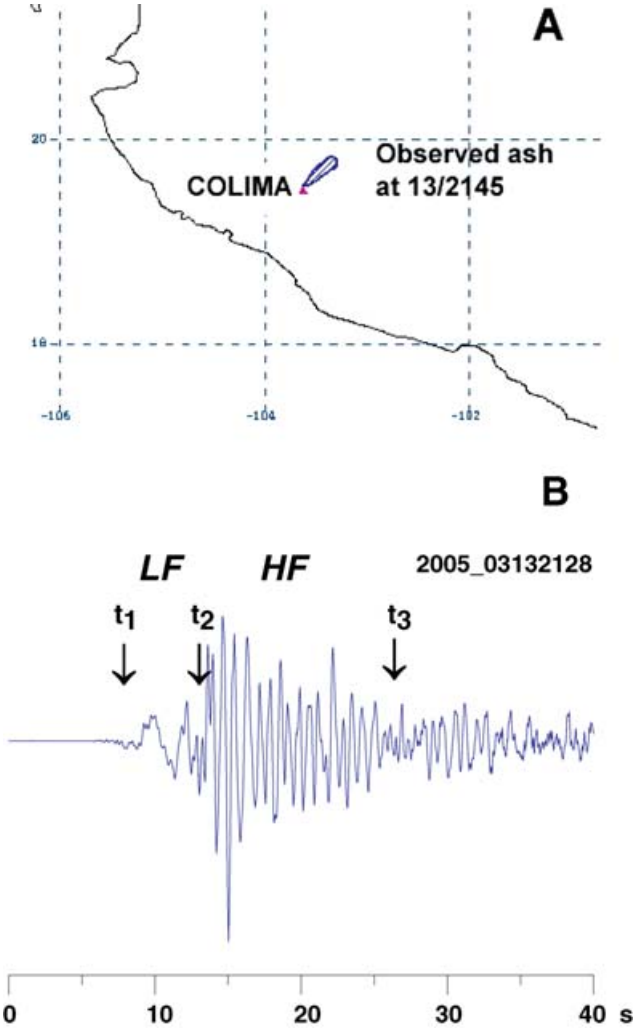

Figure 1. Seismic broad-band record of a Vulcanian explosion from 2005 March 13 (21:28 UT) at Volcán de Colima, Mexico. A. The VAAC, Washington satellite image of an ash cloud developed after the explosion. A triangle shows the position of Volcán de Colima; A shaded oval shows the area of ash cloud. B. The unfiltered vertical component of velocity corrected for instrument response recorded at a distance of 4 km from the crater. The moments of the beginning of the LF impulse (t_1), and of the beginning (t_2) and the end (t_3) of the HF impulse are indicated. LF is a low-frequency impulse; HF is a high-frequency impulse.

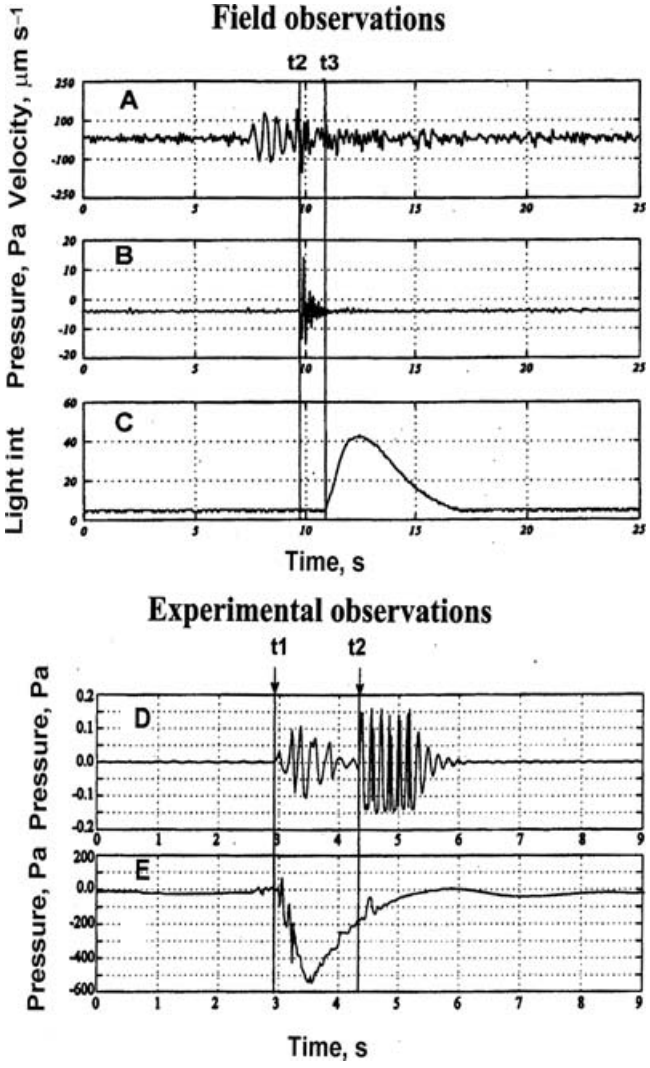

Figure 2. Basic data for the model of an explosion earthquake (field and experimental observations). Field observations: seismic (A), infrasonic (B) and light sensitive (C) recordings of the Stromboli explosion of July 11, 1994. Experimental observations: (D) sensor outside the water in the tube records a LF signal during the movement of a gas slug to the surface; the HF signal appears when the bubble film breaks at the water surface. (E) Sensor inside the water records a strong decompressive signal during the slug movement. The moments of the beginning of the LF impulse (t_1), of the beginning of the HF impulse (t_2) and the surface manifestation of explosion (t_3) are indicated. Taken from Ripepe et al. (2001; Figs 10 and 12) with some modifications.

station networks situated close to the active crater of volcanoes Stromboli, Italy, Erebus, Antarctica and Popocatépetl, Mexico. Chouet *et al.* (2003, 2005) used VLP signals recorded at Stromboli and Popocatépetl to estimate the source-centroid location and source mechanism represented by the moment tensor and the 3-D single-force vector. These signals differ from the records of larger explosions like those shown in Fig. 1 and describe the seismic response to very small explosive events recorded at a very close distance to the crater.

Our paper develops a methodology for the seismic quantification of volcanic explosions. We obtain a set of three parameters for volcanic explosive events: the magnitude of the counter force of the eruption obtained from the modelling of the LF impulse, the time for the movement of the gas bubble to the surface and the power of explosion derived from the HF impulse of the seismic record, which gives the characteristics of the process as well as the size of explosive eruption. We use the broad-band records of a 2004–2005 sequence of volcanic explosions at Volcán de Colima, Mexico, to demonstrate the application of this methodology.

2 THE CONCEPTUAL MODEL OF SEISMIC PROCESS ASSOCIATED WITH A VOLCANIC EXPLOSION

Field observations of small explosions at the basaltic (Bertagnini *et al.* 2003) Stromboli volcano by seismic and acoustic sensors (Chouet *et al.* 1997) showed that the beginning of a HF impulse recorded by a broad-band sensor coincides with the arrival of infrasonic waves that interfere with the initial LF signal (Fig. 2). The acoustic signal appears some seconds later after the arrival of the

HF signal. The visible explosion, indicated by the sharp increase in the recording of light intensity, appears after the HF impulse is registered (Fig. 2c).

To explain the origin of LF and HF impulses in the seismic record of a volcanic explosion, Ripepe *et al.* (2001) carried out a laboratory experiment, where bubbles in water were formed by air pumped at a constant flow rate from the bottom of a cylindrical tank of Plexiglas filled with water. They merged into a pipe imitating a magma conduit. The gas foam accumulated at the roof of the tank and then collapsed into a large bubble inside the pipe. The bubble began to flow within the pipe and then finally broke at the liquid surface. During the movement of the bubble, an acoustic sensor in a tube outside the water recorded a LF signal; when the bubble breaks at the liquid surface, a HF signal was recorded (Fig. 2d). The sensor located in the water recorded a strong decompression signal during the bubble movement to the liquid surface (Fig. 2e).

The laboratory signals present strong similarities to the seismic signal of a volcanic explosion (Fig. 2). These field and laboratory experiments allowed Ripepe *et al.* (2001) to infer that the LF seismic signal was generated by the rapid expansion of gas in the magma conduit, while the HF seismic signal was generated by the explosion at the free surface of magma. Therefore, the parametrization of a volcanic explosion by seismic data may be constrained by the dynamic characteristics of both impulses and time delay between their arrivals.

This model was developed for basaltic volcanoes with a liquid magma. In this paper, we apply this model to the seismic records of andesitic Volcán de Colima. The similarity between the broad-band seismic signals produced by explosions at the basaltic volcano Stromboli and the andesitic Volcán de Colima (Figs 1 and 2) implies that in general the processes leading up to and continuing during a volcanic explosion are similar for different types of magma and the broad-band seismic signal reflects two stages in the explosive process, the movement of gas in the conduit and the explosion expressed by the LF and HF impulses.

3 METHODOLOGY OF THE QUANTIFICATION OF VOLCANIC EXPLOSIONS FROM A BROAD-BAND SEISMIC RECORD

According to the conceptual model of the seismic process, the two seismic impulses from the broad-band record were used to quantify a volcanic explosion. The size of the force that controls the movement of the gas bubble in the conduit to the surface was derived from the LF impulse and the size of the volcanic explosion was derived from the HF impulse. We develop a methodology utilizing the monitoring system of Volcán de Colima where only one broad-band station EZ5 was in operation and was situated at a distance of 4 km from the crater (Fig. 3b).

3.1 Characteristics of the low-frequency seismic impulse

A LF impulse is supposed to be generated by the rapid expansion of gas in the magma conduit (Ripepe *et al.* 2001). The process of expansion of the gas (or degassing) may be thought of as a vertical movement of gas bubbles; as the slug rises and expands, liquid magma moves downward to fill the void left behind the escaping gas. Reaching the free surface of magma, the slug explodes producing the eruption. The pressurized gas exerts an impulsive upward vertical force F that is considered as the counter force of the eruption

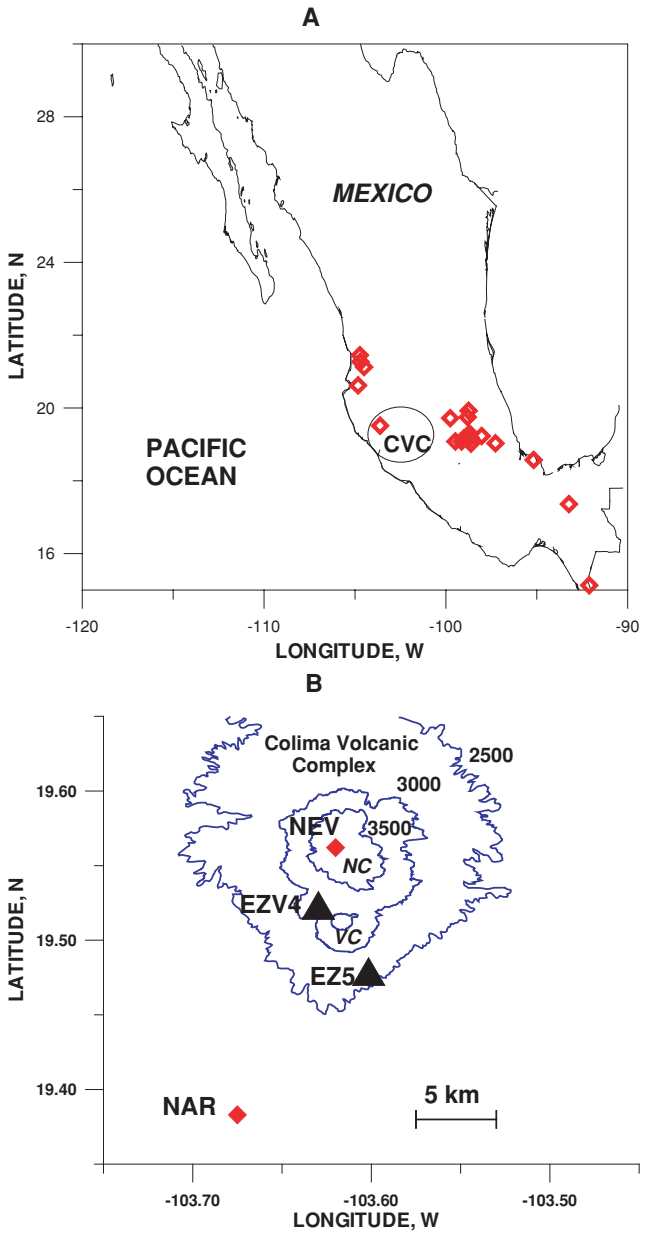

Figure 3. Position of Colima Volcanic Complex (CVC) within the Trans-Mexican Volcanic Belt (A) and the system of monitoring of the volcanoes of CVC (B). In A, the active volcanoes are shown by open diamonds. The oval shows the position of CVC. In B, the contour lines at 2500, 3000 and 3500 m show the relief of the CVC. VC is Volcán de Colima; NC is Nevado de Colima. The seismic stations EZ5 and EZV4 are shown as triangles; the video stations NAR and NEV are shown as diamonds.

(Kanamori *et al.* 1984). This counter force of the eruption may be introduced into the framework of the foam collapse model (Jaupart & Vergniolle 1990; Ripepe *et al.* 2001).

The counter force of the eruption F may be calculated from the modelling of the LF impulse recorded by a single station or by a network (Kanamori *et al.* 1984; Nishimura & Hamaguchi 1993). Kanamori & Given (1983) showed that the counter force of an eruption can be estimated considering the seismic record of the eruption as a Lamb‘s impulse produced by a vertical force and consisting of a small impulse of the body waves and an intensive impulse of a Rayleigh wave. To estimate the counter force of an eruption that

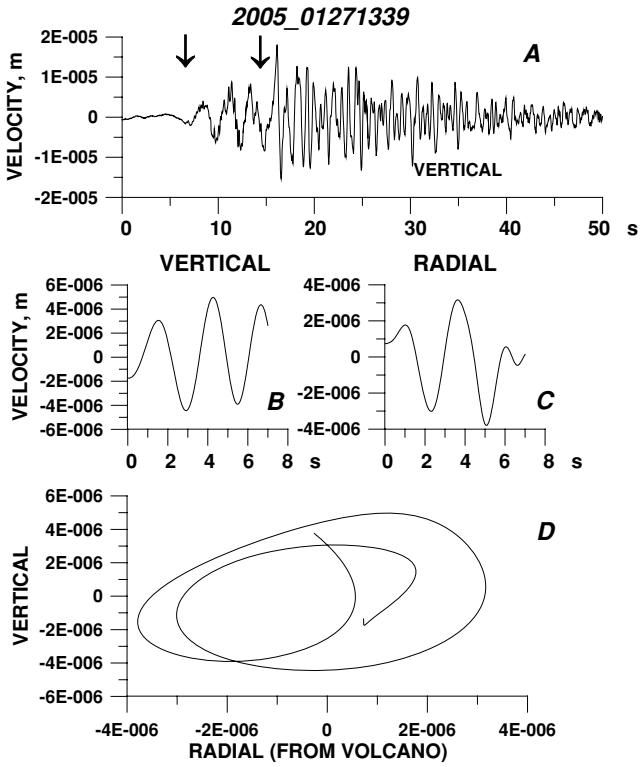

Figure 4. Particle motion in the record of the LF impulse. A, the seismogram (vertical component); the LF impulse is marked by arrows. B and C, the vertical and radial components of the LF impulse were low-pass filtered at 0.5 Hz. D, the trajectory of retrograde particle motion.

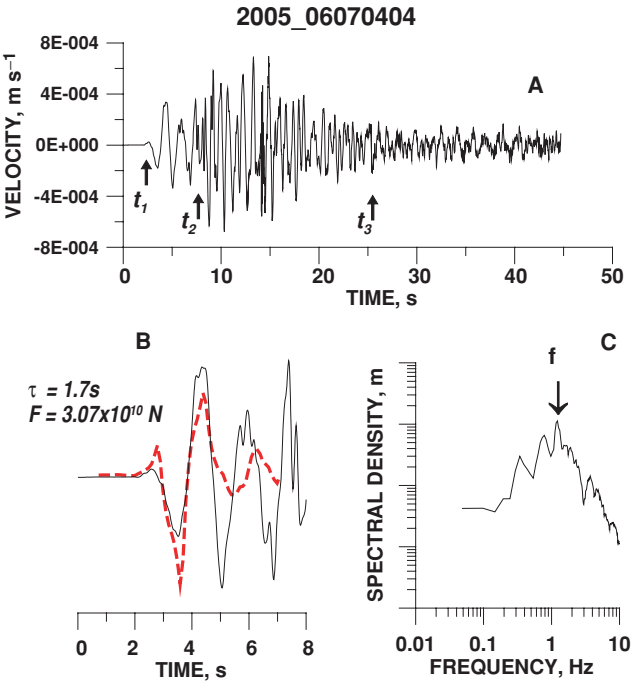

Figure 5. Illustration of the processing of seismic signals. The broad-band unfiltered seismic signal (vertical component of velocity) corrected for instrument response is shown in A. The time indices t_1, t_2, and t_3 indicate the beginning of the LF impulse, the beginning of the HF impulse, and the end of the HF impulse, respectively. The modelling of LF signal is shown in B. The dashed line shows the synthetic seismogram; the solid line is the observed seismogram. The Fourier spectrum of the HF velocity impulse is shown in C. The position of the peak frequency f is shown by arrow.

produces a LF impulse, it is necessary to show that this impulse is represented by a Rayleigh wave and to calculate a synthetic seismogram, modelling the LF impulse.

3.1.1 Wave nature of a low-frequency seismic impulse

Fig. 4 shows the particle motion for a LF impulse. To avoid the influence of HF noise, the records of vertical and radial components were low-pass filtered at 0.5 Hz. The record is short but it is possible to see that the retrograde motion of particles forms well-expressed ellipses in the vertical plane that is characteristic for Rayleigh waves (Bullen & Bolt 1985).

3.1.2 Modelling of the LF seismic impulses

The Rayleigh nature of seismic waves allows us to use the methodology of modelling a LF impulse as a Lamb's impulse with the estimation of a counter force of the eruption (Kanamori & Given 1983). To determine a counter force of an eruption at Volcán de Colima, we calculated the time domain synthetic seismograms (vertical component) excited by a single vertical impulse of a unit force F (1 N) originating at a depth 0.5 km below the crater of the volcano and recorded at a distance of 4.0 km. The distance of 4 km was the distance to the seismic station EZ5 (Fig. 3). The depth of the source of the LF impulse is a problematic value. According to Ripepe *et al.* (2001), the source of a LF impulse is the vibration of a magma conduit during the movement of a gas slug to the surface. Therefore, it has a changing depth. So we consider the depth as the initial point of the slug rise and it is not the depth of the following explosion. The depth of 0.5 km was taken based on the mean depths estimated for the explosions that occurred at the 5452-m-high andesitic Popocatépetl volcano (Cruz-Atienza *et al.* 2001). Having only one station, we could not constrain the depth of the explosion by modelling.

For the calculation of synthetics we used codes by Nishimura (1995). These codes were prepared by applying the discrete wavenumber method by Bouchon (1979, 1981) and the reflection and transmission coefficient matrices (Kennett & Kerry 1979). The source time function was taken as a triangle with a pulse width τ. The three-layer crust structure used for modelling was taken from (Nuñez-Cornú *et al.* 1994) with some simplifications. The model does not take into account the topography of a volcano.

The procedure by Nishimura (1995) does not include any technique of inversion (such as least-square iterations) for precise comparison of synthetic and observed records. At the same time, the simple form of the synthetics allows us to do a visual comparison of the records with the modelled synthetics with different τ values (Fig. 5b). We estimate the values of F and τ selecting an impulse with τ that has the same width as the observed impulse and normalizing the synthetic and observed impulses.

Our assumptions about the fixed depth and some simplifications of Nishimura's procedure such as the absence of topography effect and the visual comparison of the records do not allow absolute values better than ± 0.5 log unit. At the same time, this methodology can give us F for a sequence of explosions at the same volcano with a relative precision of about ± 0.1–0.3 of a log unit.

3.2 Characteristics of the high-frequency seismic impulses

The HF impulse is supposed to be generated by the explosion of the gas slug near a free surface of magma covering the magma conduit (Ripepe *et al.* 2001). This process may be characterized by a volumetric tensor (Kanamori *et al.* 1984; Chouet *et al.* 1997). We have only one broad-band seismic station, a situation that does not allow the reconstructing of this tensor. Therefore, we introduce the parameter of apparent power of an explosion *Pa* considering it as the energy of the seismic impulse calculated from the Fourier spectrum of the velocity impulse according to Parsival's theorem (Weaver 1983) and divided by the time of duration of the HF impulse ($t_3 - t_2$) corresponding to the duration of an explosion (Fig. 5). We also consider the peak frequency f of the spectrum.

3.2.1 Estimation of the apparent power of explosions

The theorem of Parsival (Weaver 1983) states that it is possible to calculate the total amount of energy E (for the unit of mass) in a continuous signal v(velocity) from the Fourier spectrum of the signal:

$$E = \int_0^{2\pi} v^2(t)\,dt. \tag{1}$$

According to this theorem, we calculate the apparent energy *Ea* (in Joules) of the HF impulse as the integral (1) where v is the length of the Fourier vector taken from the minimum to maximum frequencies of the spectrum. The value *Ea/t*, where t is the duration of HF impulse $t_3 - t_2$ (See Fig. 5a), gives us the value of the apparent power of the explosion *Pa* (in Watts) representing the proportion of the total power of the explosion that is contained in the seismic signal.

We consider that the apparent power of an explosion is

$$Pa = p \times k \times P, \tag{2}$$

where p is the coefficient of the seismic portion of the total energy of an explosion and k is the coefficient of effective attenuation of seismic energy with distance including the effects of geometrical spreading, energy absorption, focal mechanism and station conditions. For a fixed seismic station, p and k may be proposed as constant. Then, the apparent power of an explosion *Pa* measured at a fixed seismic station would be a value proportional to the total power of an explosion and would serve as a size value of explosions for their comparable study and quantification.

3.2.2 Estimation of the power of explosions at Volcán de Colima

The coefficients p and k from eq. (2) may be approximately estimated for the explosions of Volcán de Colima recorded by the seismic station EZ5.

Pyle (2000) published the comparative estimations of the total and seismic energy release for some volcanic explosions. According to his data for the 1980 eruption of Mount St. Helens and the 1991 eruption of Pinatubo, the coefficient of the seismic portion of the total energy of an explosion p is about 10^{-5}.

The coefficient of effective attenuation of seismic energy with distance k may be estimated from the relationship between the total seismic energy of earthquakes and the apparent seismic energy of the signal recorded at seismic station EZ5. The magnitudes of two earthquakes produced by the explosions of 2005 June 2 and 5 at Volcán de Colima were estimated by the National Seismic Survey of Mexico as 4.1 and 4.2, respectively. This gives the seismic energy of these events as 7×10^8 *J*, according to the Gutenberg–Richter relationship between the magnitude *mb* and seismic energy of earthquake

$$\mathrm{Log}E(\mathrm{ergs}) = 5.8 + 2.4\,mb. \tag{3}$$

The apparent seismic energy of these events was equal to 3.63×10^{-6} *J* and 1.46×10^{-5} *J*, respectively. Therefore, the apparent coefficient k is approximately equal to 10^{-13}. Finally, we have the following equation for estimation of energy and power of explosions at Volcán de Colima:

$$E = 10^{18} \times Ea; \quad P = 10^{18} \times Pa. \tag{4}$$

The eq. (4) can give us the values of E and P with a precision of about half an order of magnitude. At the same time, the estimations of E and P for a sequence of explosions at the same volcano can give a resolution of about ± 0.1 of log unit.

4 QUANTIFICATION OF THE 2004–2005 EXPLOSIVE ERUPTIONS AT VOLCÁN DE COLIMA, MEXICO

The described methodology was applied to quantify the explosive eruptions that occurred at Volcán de Colima, Mexico in 2004–2005.

4.1 Volcán de Colima and its activity in 2004–2005

The andesitic, 3860 m high, stratovolcano Volcán de Colima is one of the most active volcanoes in Mexico. It is located in the western part of the Mexican Volcanic Belt, and together with the Pleistocene volcano Nevado de Colima, forms the Colima Volcanic Complex (CVC) (Fig. 3). Volcán de Colima displays a wide spectrum of eruption styles, including small phreatic explosions, major block-lava effusions, and large explosive events (Breton Gonzalez *et al.* 2002). The most recent unrest at Volcán de Colima began on 1997 November 28 with a sharp increase in seismic activity and a significant shortening of geodetic lines around the volcano. This then developed into three stages of activity during the period 1998–2005. Each of these stages consisted of the extrusion of andesitic block-lava with the formation of lava flows and a lava dome and the following destruction of the lava dome by a sequence of explosions (Zobin *et al.* 2002, 2005, BGVN 1980–2005).

The most recent stage of eruptive activity at Volcán de Colima began on 2004 September 30. The extrusion of andesitic lava, that occurred in 2004 September–November, formed two lava flows of about 2400 m long and about 300 m wide and of about 600 m long and 200 m wide, on the N and WNW flanks, respectively. The total volume of erupted material including lava and pyroclastic flows was calculated taking the area of flows from photographs and considering a mean thickness of lava flow equal to 25 m. It gave the total amount of about 8.3×10^6 m^3. The lava effusion was accompanied and followed by intermittent explosive activity represented mainly by small steam-and-ash Vulcanian explosions. With the termination of lava effusion, the number of small explosions gradually decreased during 2004 December–2005 January, staying at a rather stable low level in 2005 February–June (Fig. 6). Comparatively large explosions began to occur starting 2005 March 10. The largest, accompanied by pyroclastic flows, were particularly vigorous from May 24 to June 5. Some of these explosions

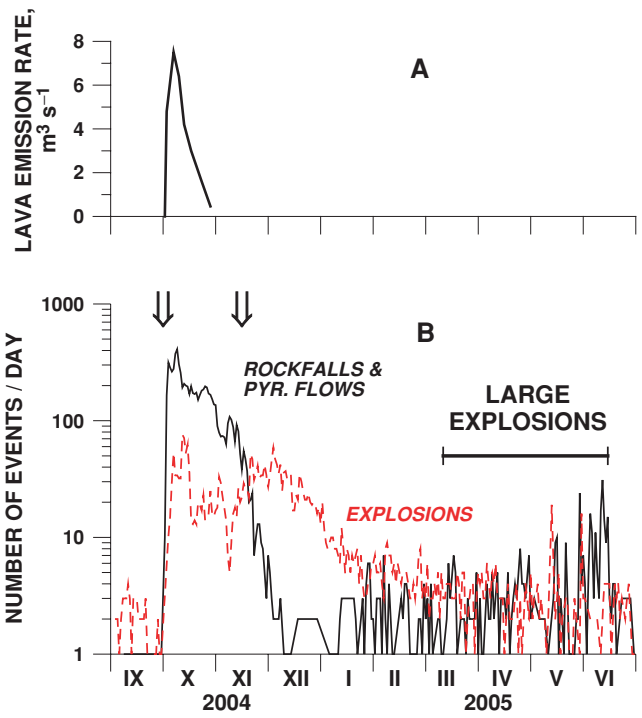

Figure 6. Characteristics of eruption activity of Volcán de Colima in 2004 September–2005 June. (A) Variations in the rate of lava emission; (B) Variations in the number of earthquakes produced by rockfalls and pyroclastic flows (heavy line) and by explosions and exhalations (dashed line) calculated from the short-period seismic records at seismic station EZV4 (See Fig. 3) situated at a distance of 1.7 km from the crater. Arrows show the beginning and the end of active lava extrusion; the interval of large explosions is shown.

issued material that reached an altitude as high as 10 km, and pyroclastic flow run-out distances reached up to 5.1 km. The March–June explosive sequence removed the 2004 lava dome, and left a crater 260 m across and 30 m deep (Fig. 7) having emitted volcanic material with a volume of about 2×10^6 m^3. The altitude of the volcanic columns and the total volume of erupted material mean that a value of the VEI = 2 can be attributed to the 2004–2005 eruption.

4.2 System of monitoring explosive activity

The system of monitoring explosive activity of Volcán de Colima was both seismic and visual (Fig. 3b). The seismic station EZ5 situated at a distance of 4 km from the crater on the southern flank of the volcano was equipped with a broad-band three-component GURALP CMG-40TD sensor with a corner frequency of 30 s and a digitizer DM24 with a sampling rate of 100 samples s^{-1} and a short-period (Ts = 1 s) vertical sensor. It was used for the analysis of the seismic signals of explosions. The short-period vertical-component seismic station EZV4 situated at a distance of 1.2 km from the crater was used for a count of seismic events of different types.

Sony model CCD-TRV118 infrared videocameras were installed at two sites (Fig. 3b): 15 km S from the crater (NAR) and 5.5 km N of the crater (NEV). They worked in a continuous regime and took automatically four digital pictures each minute. They were not synchronized exactly with seismic timing and their images were used only for identification of surface outbreaks during the explosions at the volcano.

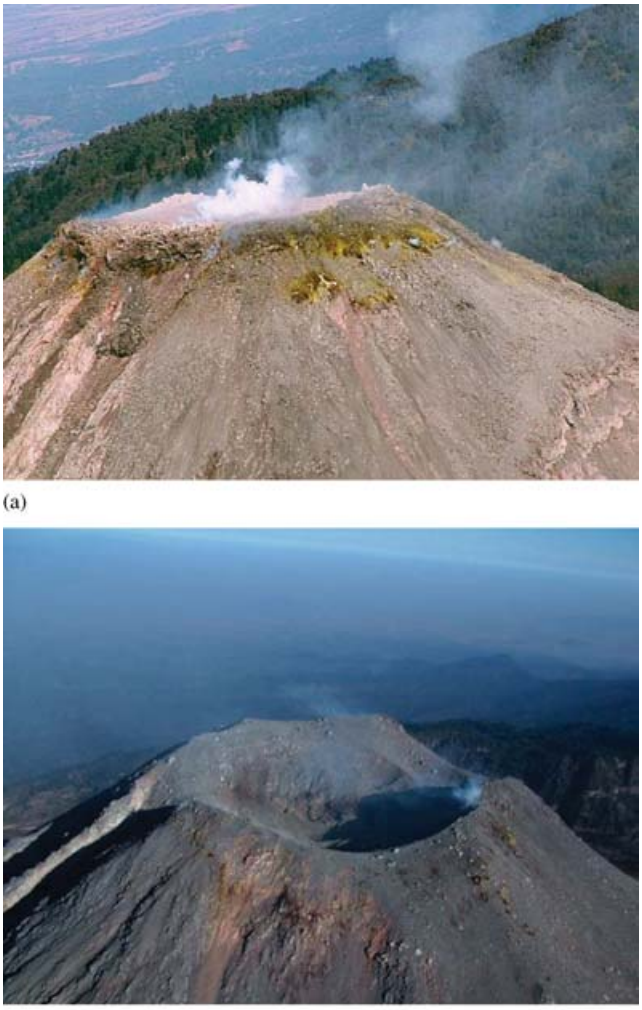

Figure 7. Photographs of the crater of Volcán de Colima showing the lava dome formed in 2004 November–December (taken on 2004 December 8) and the crater formed after the 2005 March–June explosions (taken on 2005 June 16). The photographs were taken by C. Navarro. Courtesy of Colima Volcano Observatory.

4.3 Description of seismic signals

The seismic signals were selected after a preliminary inspection of the video images recorded at NEV and NAR locations (Fig. 3). Only seismic records associated in time with a good-looking eruptive column were selected. Fig. 8 shows four main types taken from the broad-band records of explosive events. The seismograms are similar considering the form of the HF explosive impulse but differ in the form of the LF precursor. For the first three types of seismograms, we had three-, two- and one-impulse LF records; for the fourth type, the LF impulse is absent. VLP events were not recorded by our broad-band station.

Hereafter, we shall consider in our analysis two groups of seismic signals: the first, with the significant presence of the LF impulse (following the accepted model, with the preliminary movement of a gas slug in the magma conduit to the surface of the magma body) and the second, practically consisting only of a HF impulse. In our

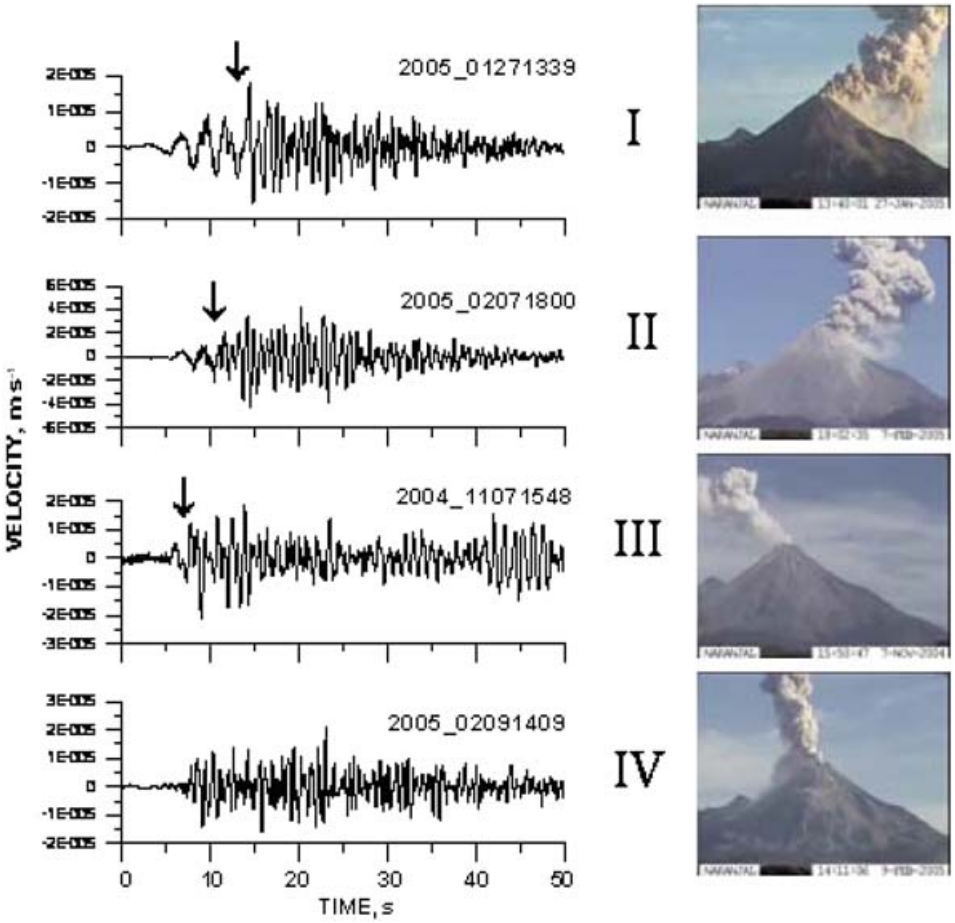

Figure 8. Four types of seismic records of explosions and corresponding video images recorded at NAR. Type I is characterized by three LF impulses; type II, by two; type III, by one and type IV, without LF impulse. Arrows show the end of LF impulse.

study, we use 66 events of the first group and 50 events of the second group.

5 SEISMIC PARAMETRIZATION OF THE 2004–2005 EXPLOSIVE PROCESS AT VOLCÁN DE COLIMA

5.1 Processing of seismic signals

Fig. 5 shows the processing of the unfiltered broad-band seismic signals. The vertical component of velocity corrected for instrument response was used. The LF and HF impulses were visually discriminated. The LF impulse was taken between the first arrival of the signal (t_1) and the beginning of the HF vibrations (t_2). The precision of the measurement of the arrival time (t_1) was about ± 0.1 s; the precision of measurement of t_2 was about ± 0.5 s. The three- and two-impulses LF precursors were modelled to estimate the counter force of the eruption (Fig. 5b).

The HF velocity impulse was taken within a time interval of $t_3 - t_2$, where t_3 was considered as the end of the vibrations generated by the explosion. The precision in the selection of this moment as the end of vibrations was not better than 1 s. Then the HF impulse was transformed into the frequency domain by the Fast Fourier transformation (Fig. 5c). Calculation of the energy of the seismic impulse followed (according to Parsival's theorem) and selecting the peak frequency of the spectrum f.

For the seismograms of the three first types, the duration of LF precursor (or time delay of the second impulse) was measured as $D = t_2 - t_1$.

The counter force of the eruptions and the power of explosions were estimated for 66 events of the first group (Table 1); the power of explosion was estimated also for 50 smaller events of the second group.

5.2 Characteristics of calculated parameters

5.2.1 Parameters of the moving slug of gas

Fig. 9 shows the distribution of the counter forces of eruptions F against the pulse width of the source time functions τ inferred from the modelling. The estimated values of F vary from 8.3×10^7 to 8.4×10^{10} N while the values of τ vary from 0.7 to 3.6 s. These values are not correlated at the 99 per cent significance level. It is possible to distinguish two groups of events according to this distribution of F versus τ: strong events with the values of F between 10^{10} and 10^{11} N and weak events with the values of F between 10^8 and 10^{10} N.

The duration of an LF impulse indicates the time taken by the gas slug to rise to the free surface of magma and varies for these events from 2.2 to 10.3 s. Fig. 10 shows that the size of a counter force does not depend on the duration of gas slug passage to the free surface of magma (the coefficient of correlation $R = 0.02$).

Table 1. Seismic characteristics of the explosive events of the first group (type 1 and 2).

Date, yyyy_mmddhhmm	τ, s	F, N	D, s	f, Hz	P, W
2004_10181257	1.28	7.08E+08	2.3	0.82	2.41E+08
2004_10311529	2.73	2.01E+09	5.6	1.27	1.17E+09
2004_11011723	1.66	1.77E+09	2.9	1.6	8.71E+08
2004_11031310	1.50	8.69E+08	9.3	1.74	7.48E+07
2004_11031652	1.80	8.17E+08	5.6	0.79	6.80E+06
2004_11111544	1.85	9.16E+08	8.2	1.32	3.82E+07
2004_11171559	1.30	1.71E+09	2.7	1.22	6.81E+08
2004_11231818	2.10	1.74E+09	4	0.85	5.74E+07
2004_11251223	2.15	4.18E+09	4.3	1.27	2.90E+08
2004_12010007	2.60	5.24E+08	8.3	0.96	1.59E+08
2004_12011346	1.30	3.79E+08	6.1	1.32	8.95E+07
2004_12141533	1.40	2.89E+08	4.5	0.94	1.64E+07
2005_01012348	1.60	5.43E+08	5	1.32	8.93E+07
2005_01021356	2.90	7.18E+08	4	1.6	1.39E+07
2005_01041605	1.92	6.84E+08	4.3	0.92	3.16E+07
2005_01042136	1.30	7.2E+08	3.3	1.27	3.68E+07
2005_01051351	1.83	8.4E+08	6.2	1.27	4.31E+07
2005_01061443	2.30	1.51E+09	3.6	1.17	3.59E+07
2005_01062037	2.00	9.17E+08	9.4	1.27	2.16E+08
2005_01082121	2.62	1.15E+09	9	0.96	5.11E+07
2005_01090321	2.40	3.45E+08	7	1.32	7.00E+07
2005_01101617	2.20	4.96E+08	6.3	1.04	4.64E+07
2005_01101618	0.70	83438151	2.2	1.32	6.82E+06
2005_01101640	2.20	1.07E+09	5.1	1.17	2.70E+07
2005_01251400	2.40	1.63E+09	10.3	1.13	1.13E+07
2005_01261400	2.50	2.54E+08	8.4	0.85	9.77E+06
2005_01270551	2.10	1.2E+09	5.5	1.43	4.34E+07
2005_01271339	2.80	1.35E+09	8.4	1.22	2.76E+07
2005_02022125	2.10	3.44E+09	4.5	1.32	9.72E+07
2005_02071800	2.40	1.98E+09	4.7	1.17	1.54E+08
2005_02132202	2.00	2.01E+09	6.1	1.27	1.05E+09
2005_03011659	1.80	7.27E+08	5.4	1.43	2.42E+08
2005_03020313	2.10	4.94E+08	6.4	1.08	6.25E+06
2005_03101409	1.80	1.7E+10	3.4	1.32	7.21E+10
2005_03112239	2.00	1.11E+09	3.8	1.27	4.18E+07
2005_03132128	2.20	4.72E+10	3.9	1.22	6.68E+10
2005_03260340	1.90	2.65E+10	3.5	1.22	1.17E+10
2005_04011237	2.10	3.45E+08	5.3	0.85	8.89E+06
2005_04012357	3.00	2.23E+09	5.4	0.76	3.35E+07
2005_04031620	2.20	7.2E+08	4.1	1.43	4.10E+07
2005_04051948	2.10	8.33E+08	4.3	1.43	3.57E+07
2005_04061714	2.30	2.77E+09	4.6	1.8	3.96E+07
2005_04062219	1.60	3.12E+08	2.9	1.22	1.33E+07
2005_04072142	3.00	2.47E+09	6.8	1.22	5.79E+07
2005_04090453	2.40	8.33E+08	4.4	1.27	1.58E+07
2005_04091545	1.60	7.58E+08	4.2	1.13	3.33E+07
2005_04102136	3.10	1.94E+09	5.9	0.79	8.20E+07
2005_04171259	2.00	1.09E+09	4	0.79	1.02E+07
2005_04200156	3.60	2.9E+10	7	0.76	2.16E+10
2005_04201204	2.00	5.94E+08	4.2	1.13	6.95E+06
2005_04261121	2.00	4.14E+08	4.1	1.27	9.76E+06
2005_04271743	2.50	2.06E+09	6.8	0.96	2.21E+07
2005_04292302	1.90	1.46E+09	6.6	0.89	7.32E+07
2005_05012327	2.60	1.08E+09	4	1.13	8.29E+08
2005_05052131	2.50	1.66E+09	4.2	0.89	3.54E+07
2005_05101415	2.30	4.51E+10	5.7	1.22	4.72E+10
2005_05160201	2.50	2E+10	5.5	1.00	9.86E+10
2005_05240009	1.60	2.55E+10	5.8	0.76	2.18E+11
2005_05300826	1.90	4.64E+10	2.7	0.79	4.51E+11
2005_06020449	2.20	5.47E+10	5.7	1.27	1.73E+11
2005_06030326	2.00	5.2E+08	6	1.37	9.33E+06
2005_06051920	3.00	8.42E+10	6	1.27	7.30E+11
2005_06070404	1.70	3.07E+10	4.6	1.22	5.30E+10
2005_06100254	1.60	2.59E+10	6	1.37	1.88E+10
2005_06102056	2.10	1.25E+09	5.2	0.92	1.09E+07
2005_06130144	2.50	7.06E+08	5.9	0.85	1.00E+07

Note: τ is the pulse width of the source time function; F is a counter force; D is the duration of the LF impulse; f is the peak frequency of the HF impulse spectrum; P is the power of explosion.

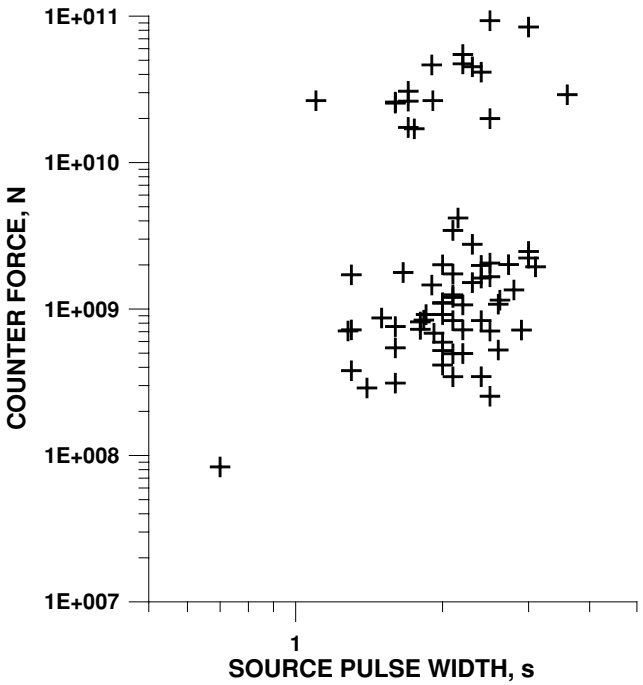

Figure 9. Relationship between the counter force of eruption F and the pulse width τ of the source time function for the 2004–2005 explosive events of Volcán de Colima.

5.2.2 Energetic parameters of volcanic explosions

Fig. 11 shows a plot of the energy of explosions E against the duration time of the HF signals t. Lines of equal power of the explosion $P = E/t$ are shown also. It varies in a broad range, between 10^6 and 10^{12} W. It is possible to distinguish the high-power explosions (P-interval from 10^{10} to 10^{12} W) from the low-power explosions. For low-power explosions, a wider interval of signal duration is characteristic, from 15 to 70 s. The low-power events include all explosive events with a short duration of gas expansion or with the absence of this process (types III and IV). All high-power events are characterized by rather short signal duration (up to 30 s).

5.2.3 Spectral properties of the high-frequency seismic impulses

The velocity spectra of the HF seismic impulses are single-peaked (Fig. 5c). Fig. 12 shows the distribution of the peak frequencies of the HF seismic impulses for two groups of our events, characterized by the presence of the LF impulse (heavy line) and practically without it (dashed line). It is possible to see that their distributions are similar having peaks at 1.2 Hz. It indicates a similar nature of explosions of all four groups as indicated in Fig. 8.

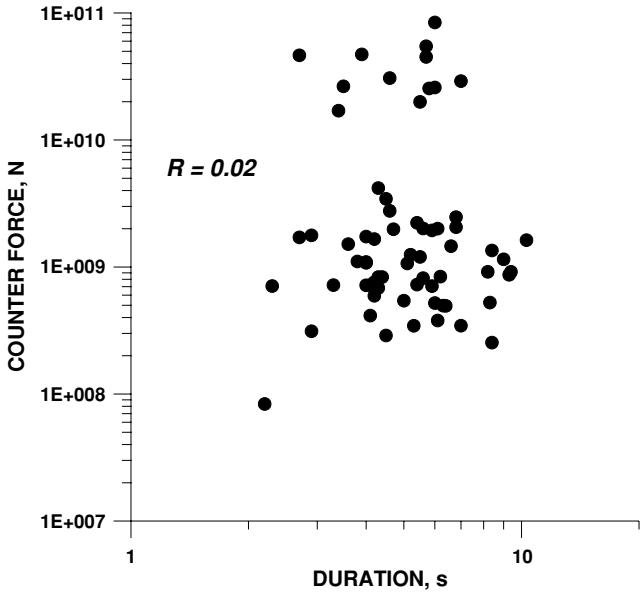

Figure 10. Relationship between the duration of the LF impulse and the counter force of the eruption. *R* is the coefficient of correlation.

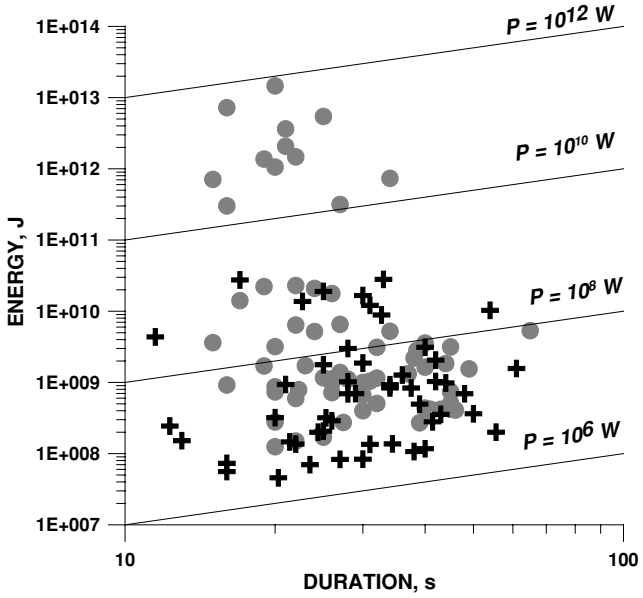

Figure 11. Relationship between the energy of explosions at Volcán de Colima and the duration of HF impulse. Lines of equal power are shown. The filled circles show the data for the first group of events; the crosses show the data for the second group of events. The definition of the groups is given in Section 4.3.

5.2.4 Relationship between the counter force of eruption and the power of explosion

Fig. 13 shows the relationship between the counter force of the eruption and the power of the explosion. These two parameters of the explosive process at the volcano are well correlated at the 99 per cent confidence level with a coefficient of correlation $R = 0.90$. The maximum likelihood regression between these two parameters is

$$\mathrm{Log}P = 2.25\,(\pm 0.06)\,\mathrm{Log}F - 12.55\,(\pm 0.56). \quad (5)$$

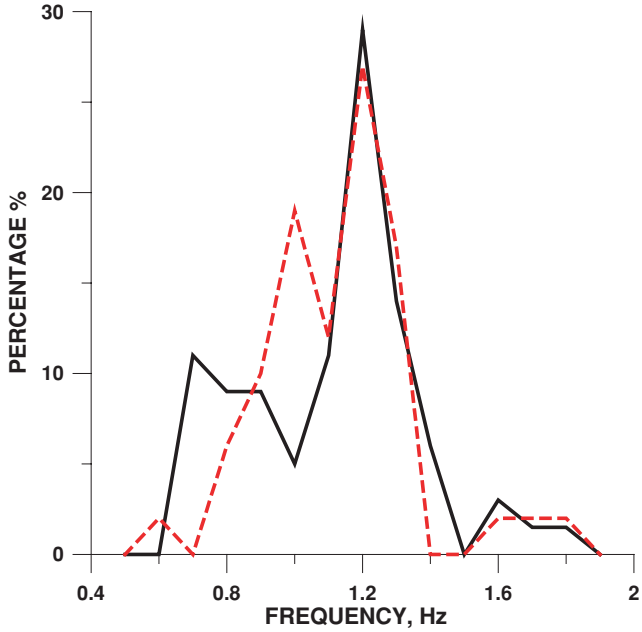

Figure 12. Distribution of the peak frequencies of the Fourier spectra of the HF impulses for the first group of events (solid line) and the second group of event (dashed line). The definition of the groups is given in Section 4.3.

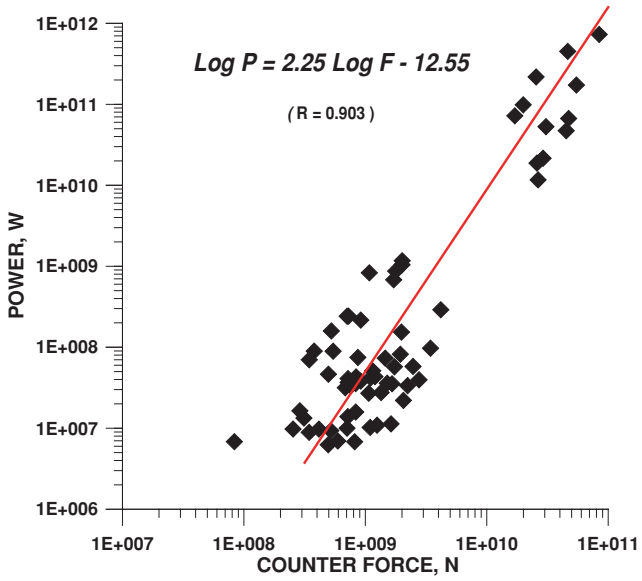

Figure 13. Relationship between the power of explosions and the counter force of eruptions. The maximum likelihood regression between these two parameters $\mathrm{Log}\,P = 2.25\,\mathrm{Log}\,F - 12.55$ is shown. *R* is the coefficient of correlation.

It shows that a power of an explosion at a volcano is directly related to the intensity of the gas slug movement in the conduit before the explosion.

Fig. 11 shows that some low-power explosions occur without a LF precursor, or without the movement of the gas slug just before the event, but all high-power explosions occur with the presence of a LF precursor in the seismic record. In the first case, we can suppose that any gas slugs that did not explode just after reaching the free surface of magma may collect there to produce an explosion later. The fact that the counter force of an eruption does not depend on the duration

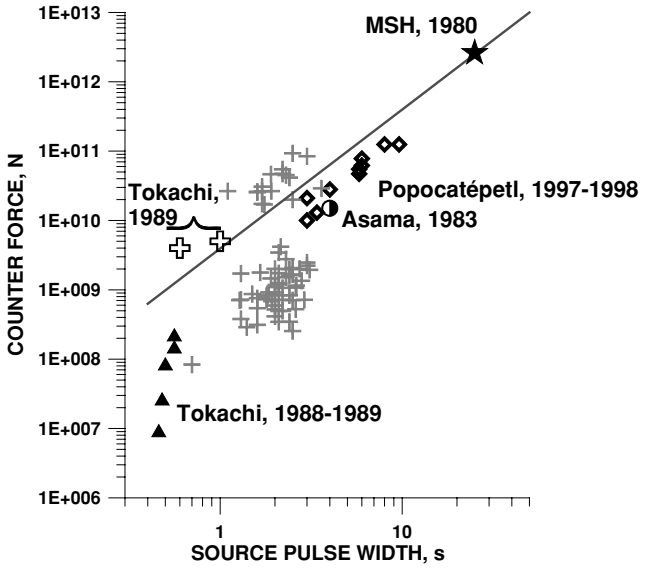

Figure 14. Relationship between the counter force of the eruption F and the pulse width of the source time function τ for the explosive events for a group of the volcanoes of the world. The data for Volcán de Colima are shown by crosses. The data for other events are shown as open diamonds (Popocatépetl, Mexico; Cruz-Atienza *et al.* 2001), open crosses (Tokachi, Japan; Nishimura & Hamaguchi 1993), a star (Mount St. Helens, USA; Kanamori *et al.* 1984), half-filled circle (Asama, Japan; Nishimura & Hamaguchi 1993), filled triangles (small events of Tokachi, Japan; Nishimura 1995). The line of scaling $\mathrm{Log}\,F = 2\,\mathrm{Log}\,\tau + 9.6$ proposed by Nishimura & Hamaguchi (1993) is shown.

D indicates this possibility. At the same time, Fig. 11 indicates that high-power explosions occurred if the size of the counter force was greater than 10^{10} N.

6 COMPARISONS BETWEEN OUR RESULTS AND OBSERVATIONS AT OTHER VOLCANOES

6.1 Scaling of the force characteristics of volcanic eruptions

The counter forces of explosive eruptions estimated by different authors vary from 4.7×10^9 N for the 1989 February 6 explosion at Tokachi volcano, Hokkaido (Nishimura *et al.* 1995) to 2.6×10^{12} N for the 1980 May 18 explosion at Mount St. Helens volcano, Cascades (Kanamori *et al.* 1984). Nishimura & Hamaguchi (1993) proposed for them the following scaling law:

$$\mathrm{Log}F = 2\,\mathrm{Log}\tau + 9.6. \quad (6)$$

Fig. 14 shows that the strong explosive events of Volcán de Colima are in accordance with this scaling law. At the same time, the weak explosions of Volcán de Colima as well as the weak explosive events of Tokachi volcano, demonstrate a weaker dependence of F on τ. It supports the earlier results of Nishimura (1995) about the different source behaviour of large and small volcanic explosions.

Nishimura (1995) considers that while for stronger explosions the relation between F and τ can be characterized by F per cent τ^2, for the small Tokachi explosive events, $\tau \approx$ const. Nishimura explains this difference by the constant temperature of magma associated with the strong explosions and a variation in the temperature of magma causing the small explosive events. Our results support that the scaling of small events may differ from the scaling of stronger events but at the same time the value of τ for the small Colima events is not constant.

6.2 Power of volcanic explosions

The power of explosions at Volcán de Colima varies from 10^6 to 10^{12} W. The maximum values are comparable with the power of a hydrothermal electrical plant; the minimum, with the power of a locomotive (Benson 1991). Pyle (2000) published the values of power output from some explosive eruptions based on the thermal energy release estimated from tephra volumes. The maximum power was estimated as 10^{15} W for the ancient eruption of Taupo volcano, New Zealand. The power of gigantic explosions at volcanoes of Bezymianny, Kamchatka in 1956 and Mount St Helens, Cascades in 1980 was estimated as 2.8×10^{14}W and 2×10^{13} W, respectively.

The estimations of power for the Colima explosions are comparable with those for four 1986 explosions at Augustine volcano, Alaska which vary between 1.5×10^8 and 1.5×10^{12} W (Pyle 2000). These explosions were characterized by the height of column reaching altitudes from 800 to 8000 m a.s.l. (Pyle 2000) that are close to the height of columns associated with Colima explosions.

6.3 Characteristics of the gas slug movement to the free surface of magma

The duration of the LF impulse, $D = t_2 - t_1$, that is considered as being proportional to the time taken by the upward movement of the gas slug in the conduit to the free surface of magma was recorded at a distance of 4 km from the active crater. This varied at Volcán de Colima from 0 (for the event of type IV, Fig. 8) to 10.3 s (for the events of type I). Ripepe *et al.* (2001) wrote that the parameter D calculated for explosive events of Stromboli was not stable also but oscillated between 0.75 and 5.5 s in the records at a distance of about 300 m from the crater. The instability in size of this parameter may indicate a change in position of the initial point in the movement of the gas slug in the conduit.

This parameter D may depend strongly on the type of magma, particularly its viscosity. This aspect has not been investigated yet. Nevertheless, the analysis of temporal variations of this parameter during a sequence of explosions of a volcano could give additional information about the variation in position of the source of generation of gas bubbles.

7 THE DESCRIPTION OF A VOLCANIC PROCESS WITH A SET OF PROPOSED PARAMETERS OF EXPLOSIVE ERUPTIONS

The recent 2004–2005 eruption at Volcán de Colima developed in two stages (Fig. 15). A sharp change in the level of explosive activity at the volcano occurred in the end of 2005 January, when the effusive process was completely terminated (Fig. 15a). We can consider stage 1 as effusive-explosive activity and stage 2 as completely explosive activity.

Fig. 15(b) shows the temporal variations in the duration of the LF impulses of seismic records, which are characteristic of the process of gas slug movement to the free surface of magma. During stage 1, the duration of slug movement changed within a wide interval, from 2 to 10 s; no events without slug movement (type IV, Fig. 8) were observed. During stage 2, the duration of slug paths became shorter,

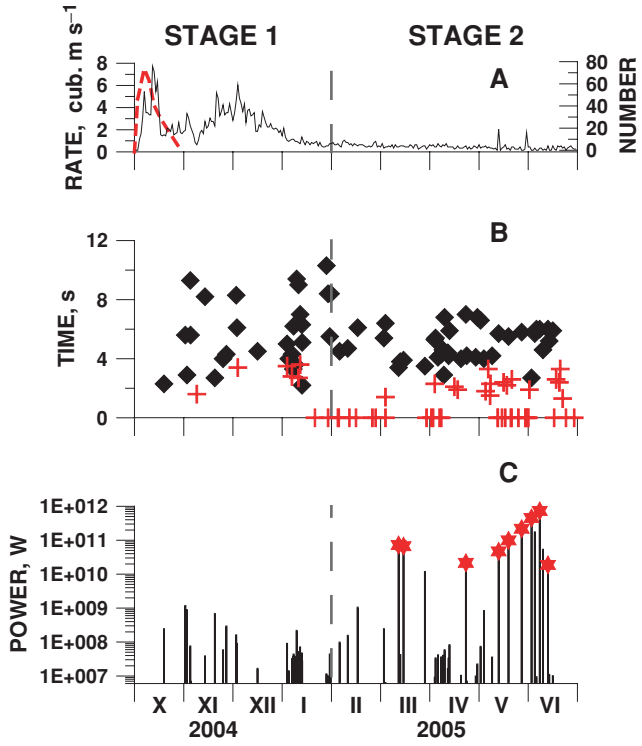

Figure 15. Variations of eruptive (A) and seismic (B, C) parameters during the 2004 October–2005 June activity at Volcán de Colima. (a) Variation in the rate of lava emission (dashed line) and in the daily number of explosive events. (b) Variation in the duration of the LF impulses. The data for the first group of events are shown by the filled diamonds; the data for the second group, by crosses. The definition of the groups is given in Section 4.3. (c) Variation in the size of power. The stars mark the explosions followed by pyroclastic flows. The vertical dashed line separates stage 1 and stage 2 of eruptive activity.

up to 6 s; many explosive events without preliminary slug movement also occurred. It indicates that during stage 1, the explosive events were generated by gas slugs that moved from a rather deep zone of the conduit. During stage 2, the depths of the initial movement of the gas slugs became shallower. A significant proportion of explosive events (type III and IV) occurred from the bubbles of gas just fixed earlier at the free surface of magma.

The occurrence of explosive events of a different size (expressed in power) is shown in Fig. 15(c). It is seen that the high-power explosions were absent during the effusive stage of the eruption. The large explosions occur only after the ceasing of lava emission.

Some explosions were accompanied by pyroclastic flows. They are marked by the stars in Fig. 15(c). It is possible to see that only the explosions characterized by a power of greater than 10^{10} W were able to generate pyroclastic flows. We had 12 explosions with this range of power in March–June; nine of them were accompanied by pyroclastic flows. The presence of pyroclastic flows for the remaining three events was not documented.

8 CONCLUSIONS

It is shown that the three parameters derived from the broad-band seismic signals may be used for the quantification of volcanic explosions: the counter force of eruption F, the power of explosion P and the duration of the gas slug movement in the conduit upward to the free surface of magma, D. During the 2004–2005 activity at Volcán de Colima, Mexico (VEI 2), the broad-band records of more than 100 explosive events were obtained at a distance of 4 km from the crater. We determined the counter force of the eruption by modelling the LF impulse of the seismic records of the volcanic explosions and estimated the power of the event from the spectra of the HF impulse. The power of Colima explosions spans five orders of magnitude; the counter force of Colima eruptions spans four orders of magnitude. More simple estimation of a power and the possibility of its estimation for all four types of explosive events shown in Fig. 8 make it preferable as a key parameter of an explosive eruption.

ACKNOWLEDGMENTS

We thank Takeshi Nishimura for providing us with the codes for calculation of synthetics. The processing of digital data was realized using the program DEGTRA provided by Mario Ordaz. The comments of Nick Varley, Tonatiuh Dominguez and two anonymous reviewers were very valuable. Nick Varley strongly improved our English grammar.

REFERENCES

Aster, R., Mah, S., Kyle, P., McIntosh, W., Dunbar, N., Johnson, J., Ruiz, M. & McNamara, S., 2003. Very long period oscillations of Mount Erebus volcano, *J. geophys. Res.,* **108,** 2522.

Benson, H., 1991. *University Physics,* **Vol. 1**. J. Wiley & Sons, New York. 521 p.

Bertagnini, A., Metrich, N., Landi, P. & Rosi, M., 2003. Stromboli volcano (Aeolian Archipelago, Italy): an open window on the deep-feeding system of a steady state basaltic volcano, *J. geophys. Res.,* **108,** 2336.

BGVN, 1980–2005. *Bulletin of Global Volcano Network,* Smithsonian Institution.

Bouchon, M., 1979. Discrete wave number representation of elastic wave fields in three space dimensions, *J. geophys. Res.,* **84,** 3609–3614.

Bouchon M., 1981. A simple method to calculate Green's functions for elastic layered media, *Bull. seism. Soc. Am.,* **71,** 959–971.

Breton González, M., Ramírez, J.J. & Navarro, C., 2002. Summary of the historical eruptive activity of Volcán de Colima, Mexico 1519–2000, *J. Volc. Geotherm Res.,* **117,** 21–46.

Bullen, K.E. & Bolt, B.A., 1985. *An introduction to the theory of seismology,* Cambridge Univ. Press., Cambridge. 499 p.

Carey, S.N. & Sigurdsson, W., 1989. The intensity of plinian eruptions, *Bull. Volcanol.,* **51,** 28–40.

Cashman, K.V., Sturtevant, B., Papale, P. & Navon, O., 2000. Magmatic fragmentation, in *Encyclopedia of Volcanoes,* p. 1417, ed. Sigurdsson, H., Academic Press, San Diego—Toronto.

Chouet, B., Saccarotti, G., Martini, M., Dawson, P., De Luca, G., Milana, G. & Scarpa, R., 1997. Source and path effects in the wave fields of tremor and explosions at Stromboli volcano, Italy, *J. geophys. Res.,* **102,** 15 129–15 150.

Chouet, B. et al., 2003. Source mechanisms of explosions at Stromboli Volcano, Italy, determined from moment-tensor inversions of very-long-period data, *J. geophys. Res.,* **108**(B1), 2019.

Chouet, B., Dawson, P. & Arciniega-Ceballos, A., 2005. Source mechanisms of Vulcanian degassing at Popocatépetl Volcano, México, determined from wave-form inversions of very long period signals, *J. geophys. Res.,* **110,** B7301.

Cruz-Atienza, V.M., Pacheco, J.F., Singh, S.K., Shapiro, N.M., Valdés, C. & Iglesias, A., 2001. Size of Popocatepetl volcano explosions (1997–2001) from waveform inversion, *Geophys. Res. Lett.,* **28,** 4027–4030.

Jaupart, C. & Vergniolle, S., 1990. The generation and collapse of a foam layer at the root of a basaltic magma chamber, *J. Fluid Mech.,* **203,** 347–380.

Johnson, J.B., Lees, J.M. & Gordeev, E.I., 1998. Degassing explosions at Karymsky volcano, Kamchatka, *Geophys. Res. Lett.,* **25,** 3999–4002.

Kanamori, H. & Given, J.W., 1982. Analysis of long-period seismic waves excited by the May 18, 1980, eruption of Mount St. Helens—a terrestrial monopole?, *J. geophys. Res.,* **87,** 5422–5432.

Kanamori, H. & Given, J.W., 1983. Lamb pulse observed in nature, *Geophys. Res. Lett.,* **10,** 373–376.

Kanamori, H., Given, J.W. & Lay, T., 1984. Analysis of seismic body waves excited by the Mount St. Helens eruption of May 18, 1980, *J. geophys. Res.,* **89,** 1856–1866.

Kawakatsu, H., Ohminato, T., Ito, H., Kuwahara, Y., Kato, T., Tsuruga, K., Honda, S. & Yomogida, K., 1992. Broadband seismic observations at the Sakurajima volcano, Japan, *Geophys. Res. Lett.,* **19,** 1959–1962.

Kennett, B.L. & Kerry, N.J., 1979. Seismic waves in a stratified half space, *Geophys. J. Res.,* **57,** 557–583.

Morrissey, M.M. & Mastin, L.G., 2000. Vulcanian eruptions, in *Encyclopedia of Volcanoes,* p. 1417. ed. Sigurdsson, H., Academic Press, San Diego—Toronto.

Neuberg, J., Luckett, R., Ripepe, M. & Braun, T., 1994. Highlights from a seismic broadband array on Stromboli volcano, *Geophys. Res. Lett.,* **21,** 749–752.

Newhall, C.G. & Self, S., 1982. The volcanic explosivity index (VEI): An estimate of explosive magnitude for historical volcanism, *J. Geophys. Res.,* **87,** 1231–1238.

Nishimura, T., 1995. Source parameters of the volcanic eruption earthquakes at Mount Tokachi, Hokkaido, Japan, and magma ascending model, *J. geophys. Res.,* **100,** 12 456–12 473.

Nishimura, T. & Hamaguchi, H., 1993. Scaling law of volcanic explosion earthquakes, *Geophys. Res. Lett.,* **20,** 2479–2482.

Nishimura, T., Hamaguchi, H. & Ueki, S., 1995. Source mechanisms of volcanic tremor and low-frequency earthquakes associated with the 1988–89 eruptive activity of Mt. Tokachi, Hokkaido, Japan, *Geophys. J. Int.,* **121,** 444–458.

Núñez-Cornú, F., Nava, F.A., De la Cruz-Reyna, S., Jiménez, Z., Valencia, C. & García-Arthur, R., 1994. Seismic activity related to the 1991 eruption of Colima volcano, Mexico, *Bull Volcanol.,* **56,** 228–237.

Pyle, D.M., 2000. Sizes of volcanic eruptions, in *Encyclopedia of Volcanoes,* pp. 263–269, ed. Sigurdsson, H., Academic Press, San Diego.

Ripepe, M., Ciliberto, S. & Della Schiava, M., 2001. Time constraints for modelling source dynamics of volcanic explosions at Stromboli, *J. geophys. Res.,* **106,** 8713–8727.

Rowe, C.A., Aster, R.C., Kyle, P.R., Schlue, J.W. & Dibble, R.R., 1998. Broadband recording of Strombolian explosions and associated very-long-period seismic signals on Mount Erebus volcano, *Geophys. Res. Lett.,* **25,** 2297–2300.

Vergniolle, S. & Mangan, M., 2000. Hawaiian and strombolian eruptions, in *Encyclopedia of Volcanoes,* p. 1417, ed. Sigurdsson, H., Academic Press, San Diego—Toronto.

Weaver, H.J., 1983. *Applications of Discrete and Continuous Fourier Analysis,* John Wiley & Sons, New York.

Zobin, V.M. et al., 2002. Overview of the 1997–2000 activity of Volcán de Colima, Mexico, *J. Volc. Geotherm. Res.,* **117,** 1–19.

Zobin, V.M., Orozco-Rojas, J., Reyes-Dávila, G.A. & Navarro, C., 2005. Seismicity of an andesitic volcano during block-lava efusión: Volcán de Colima, México, November 1998-January 1999, *Bull. Volcanol.,* **67,** 679–688.